European Review for Medical and Pharmacological Sciences 2019; 23: 3569-3574

MiR-29 regulates retinopathy in diabetic mice *via* the AMPK signaling pathway

B.-W. ZHAO, H.-Y. DAI, L.-N. HAO, Y.-W. LIU

Department of Ophthalmology, Hongqi Hospital Affiliated to Mudanjiang Medical University, Mu-danjiang, China

Abstract. – OBJECTIVE: This work aims to study the influence of micro-ribonucleic acid (miR)-29 on the retinopathy in diabetic mice *via* the adenosine 5'-monophosphate-activated protein kinase (AMPK) signaling pathway.

MATERIALS AND METHODS: A total of 24 C57BL/6 mice were randomly divided into normal group (n=12) and model group (n=12). Mice in the normal group were given to normal diet, and those in the model group were prepared for establishing diabetes mouse model. After animal procedures, electroretinogram was performed to detect the latent period and amplitude of b-wave. The expressions of B-cell lymphoma 2 (Bcl-2) and Bcl-2-associated X protein (Bax) were detected *via* immunohistochemistry. The protein levels of the phosphorylated AMPK (p-AMPK) and phosphorylated mammalian target of rapamycin (p-mTOR) were determined using Western blotting. Moreover, miR-29 expression and cell apoptosis were detected via quantitative Polymerase Chain Reaction (qPCR) and terminal deoxynucleotidyl transferase (TdT) dUTP nick-end labeling (TUNEL), respectively.

RESULTS: Compared with those in the normal group, the latent period prolonged and amplitude of b-wave decreased in the model group ($p<0.05$). Immunohistochemistry showed that compared with normal group, mice in the model group exhibited increased Bax expression and decreased Bcl-2 expression ($p<0.05$). The Western blotting analysis showed that the protein levels of p-AMPK decreased and p-mTOR increased in the model group compared with those in the normal group ($p<0.05$). The qPCR revealed that compared with the normal group, the model group had notably decreased miR-29 expression ($p<0.05$). TUNEL detection displayed that the apoptotic rate was remarkably elevated in the model group compared with that in the normal group ($p<0.05$).

CONCLUSIONS: Inhibition of miR-17-5p up-regulates the expression of VEGF-A and GDNF in MSCs, and promotes the repair of spinal cord injury by MSCs.

Key Words:
Diabetic retinopathy, MiR-29, Apoptosis, Autophagy.

Introduction

There are over 150 million cases of diabetes mellitus worldwide, and 20-45% of them suffer from diabetic retinopathy[1]. Diabetic retinopathy, a specific fundus disease, is recognized as one of the major ocular diseases causing blindness. Microangiopathy is one of the most important pathological manifestations of diabetic retinopathy accompanied by neurodegeneration[2,3]. Recent studies proposed that the neurodegeneration can occur earlier than the microangiopathy in the pathological process of diabetic retinopathy. It is reported that the blindness rate of diabetic retinopathy ranks first in the double-blind rate, which is nearly 25-fold among the non-diabetes blind population. However, the pathogenesis of diabetic retinopathy has not been fully clarified so far. Therefore, prevention and treatment of diabetic retinopathy have become urgent issues to be solved.

Micro-ribonucleic acids (miRNAs), a class of non-coding RNAs, are currently considered to play a critical regulatory role in organisms; it has been confirmed the close relation between miRNAs with the onset of multiple diseases. Studies have manifested that miRNAs degrade or inhibit the downstream messenger RNA (mRNA) through pairing with the 3' untranslated regions of downstream genes. Functionally, miRNAs exert regulatory effects on transcription and regulating cellular processes, such as proliferation, differentiation and apoptosis[4,5]. Additionally, it has been found that miR-29 is closely related to diabetes and its relative complications, and recognized as a key regulator in the pathological process of diabetic retinopathy. MiR-29 has important effects and influences on the retinopathy in diabetic mice by regulating numerous cell signaling pathways, which may be a novel therapeutic target.

This study aims to clarify the role of miR-29 in the onset of diabetic retinopathy and explore whether it exerts an effect in the disease *via* regulating the adenosine 5'-monophosphate-activated protein kinase (AMPK) signaling pathway.

Corresponding Author: Yingwei Liu, MM; e-mail: 252831514@qq.com

Materials and Methods

Laboratory Animals and Grouping

A total of 24 C57BL/6 mice weighing 20 g (12 females and 12 males) were purchased from Shanghai SLAC Laboratory Animal Co., Ltd. [License No. SCXK (Hu) 2014-0003] (Shanghai, China). Mice were randomly divided into normal group (n=12) and diabetes group (model group) (n=12). This study was approved by the Animal Ethics Committee of Mudanjiang Medical University Animal Center.

Experiment Reagents and Instruments

Primary antibodies: anti-phosphorylated-adenosine 5'-monophosphate -activated protein kinase (p-AMPK) antibody, anti-phosphorylated mammalian target of rapamycin (p-mTOR) antibody, anti-B-cell lymphoma 2 (Bcl-2) anitybody and anti-Bcl-2-associated X protein (Bax) antibody (Abcam, Cambridge, MA, USA), AceQ quantitative Polymerase Chain Reaction (qPCR) SYBR Green Master Mix kit and HiScript II Q RT SuperMix for qPCR [+genomic deoxyribonucleic acid (+gDNA) wiper] kit (Vazyme Biotech, Nanjing, China), and terminal deoxynucleotidyl transferase (TdT) dUTP nick-end labeling (TUNEL) apoptosis kit (Sigma-Aldrich, St. Louis, MO, USA), optical microscope (Leica DMI 4000B/DFC425C, München, Germany), electrophysiological instrument (Thermo Fisher Scientific, Waltham, MA, USA) and fluorescence ration PCR instrument (ABI 7500, Foster City, CA, USA).

Methods

Modeling and Treatment in Each Group

Mice in the normal group were raised with normal diet each day, and those in the model group were fed with high-fat diet for 4 weeks. Then, mice in the normal group were intraperitoneally injected with normal saline and those in the model group were injected with 100 mg/kg STZ (streptozocin), for 4 consecutive weeks. Afterward, fasting blood glucose level of mice in each group was measured. Fasting blood glucose level higher than 7.8 nmol/L indicated the successful establishment of the animal model.

Electroretinogram

After intraperitoneal injection of 7% chloral hydrate for anesthesia, each mouse was dripped with 1% atropine for mydriasis and fixed on an insulation board. Then, a reference electrode was placed on the cheek skin of mice, and a grounding electrode on the tail skin to record the latent period and amplitude of binocular b-waves.

Sampling

Mouse retinal tissues of 6 mice in each group were harvested after paraformaldehyde perfusion at 4°C for 48 h. Paraffin-embedded tissue sections were prepared for the immunohistochemistry and TUNEL detections. Retinal tissues of the remaining 6 mice were directly taken and placed in Eppendorf (EP) tubes for the detections *via* Western blotting and qPCR.

Detection via Western Blotting

Tissues were lysed on ice for 60 min, followed by centrifugation and protein quantification *via* bicinchoninic acid (BCA) assay. After the proteins were denaturalized, they were separated *via* gel electrophoresis, transferred to membranes and rinsed, followed by sealing in the blocking buffer for 1.5 h. Then, the membranes were incubated with primary antibodies of anti-p-AMPK (1:1,000), anti-p-mTOR (1:1,000) and their secondary antibodies (1:1,000). The resulting products were washed with Tris-Buffered Saline and Tween 20 (TBST), followed by color development. The membranes were placed in the chemiluminescence reagents for 1 min of reaction, followed by analysis using the gel imaging system.

Detection via qPCR

The total ribonucleic acid (RNA) was first extracted and reversely transcribed into the complementary DNA (cDNA) using a reverse transcription kit, with a 20 μL reaction system. The reaction conditions were as follows: reaction at 51°C for 2 min, pre-degeneration at 96°C for 10 min, degeneration at 96°C for 10 s and annealing at 60°C for 30 s, for 40 cycles. The relative expression levels of mRNAs were calculated with glyceraldehyde-3-phosphate dehydrogenase (GADPH) as the internal reference. The primer sequences were shown in Table I.

TUNEL Apoptosis Assay

The apoptosis in the brain tissues was detected using the TUNEL apoptosis kit according to the instructions.

Immunohistochemistry

The sections were subjected to standard dewaxing, washing in water, antigen retrieval and rinse, followed by incubation with endogenous

Table I. Primer sequences.

Name	Primer sequence
miR-29	Forward primer: 5'TCCACCAAGAAGCTGAGCGAG 3' Reverse primer: 5'GTCCAGCCCATGATGGTTCT 3'
GADPH	Forward primer: 5'ACGGCAAGTTCAACGGCACAG 3' Reverse primer: 5'GAAGACGCCAGTAGACTCCACGAC 3'

peroxidase blockers for 10 min sealing in serum for 20 min. After the sealing solution was discarded, primary antibodies of anti-Bax and anti-Bcl-2 (1:200) were added for incubation at 4°C overnight. Then, the resulting sections were rinsed and incubated with the secondary antibodies for 10 min. Subsequently, the sections were incubated in streptavidin-peroxidase solution for another 10 min, diaminobenzidine (DAB) color development (Solarbio, Beijing, China), counterstained *via* hematoxylin and sealed in neutral resin. Finally, the products were observed and photographed.

Statistical Analysis

Statistical Product and Service Solutions (SPSS) 20.0 software (IBM, Armonk, NY, USA) was employed for statistical analysis. Measurement data were expressed as mean ± standard deviation. The *t*-test was performed for data conforming to normal distribution and homogeneity of variance, corrected *t*-test for those conforming to normal distribution and heterogeneity of variance, and nonparametric test for those not line with normal distribution and homogeneity of variance. The comparison between the groups was made using One-way ANOVA test followed by Post-Hoc Test (Least Significant Difference). Rank sum test and chi-square test were conducted for ranked data and count data, respectively.

Results

Expressions of Bax and Bcl-2 Detected Via the Immunohistochemistry

Immunohistochemistry indicated stronger positive expression of Bax-2 and weaker positive expression of Bcl-2 in the model group relative to those in the control group (Figure 1). Quantitative data of Bax and Bcl-2 expressions were expressed in Figure 2.

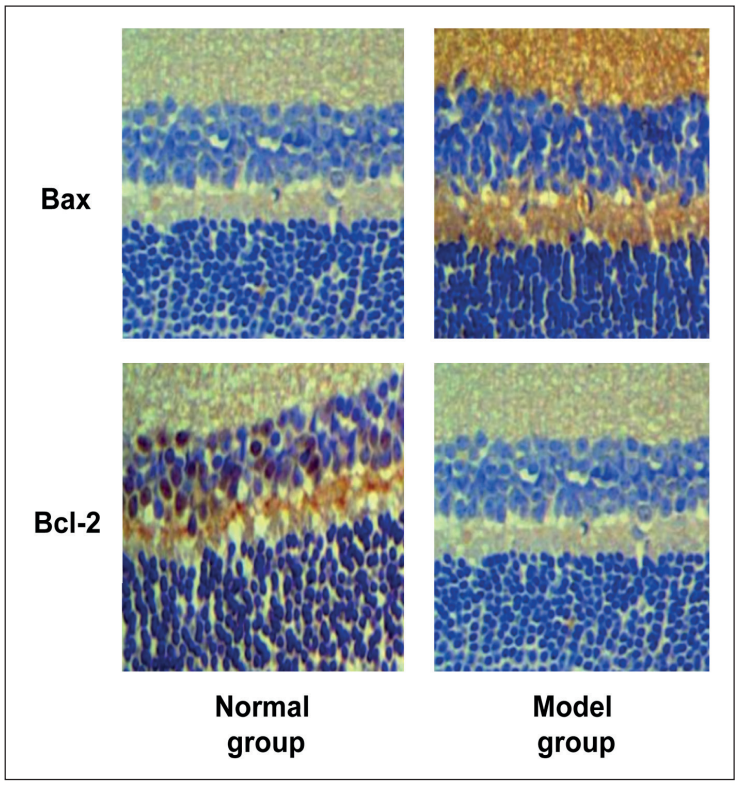

Figure 1. Expressions of Bax and Bcl-2 detected via the immunohistochemistry. (Magnification: 100×).

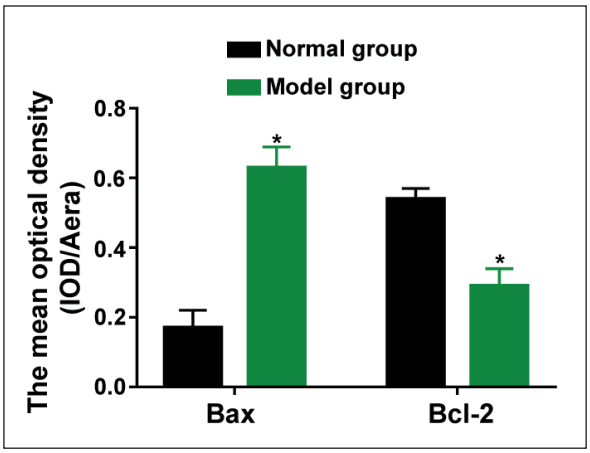

Figure 2. The mean optical density of positively expressed Bax and Bcl-2. Note: p*<0.05, *vs.* normal group.

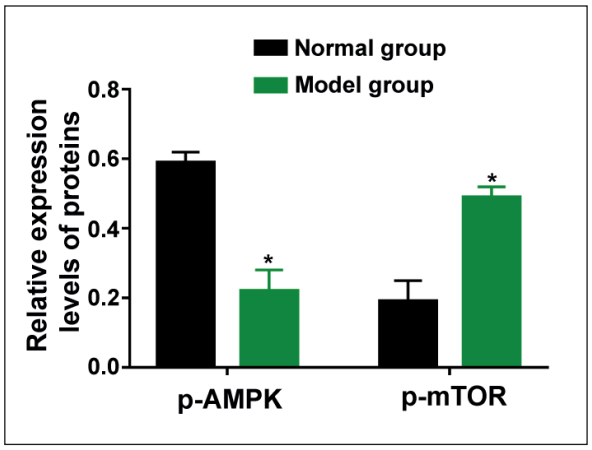

Figure 4. Relative expression levels of proteins. Note: p*<0.05, *vs.* normal group.

Relative Protein Levels of the p-AMPK and P-mTOR Detected Via Western Blotting

The normal group exhibited a higher protein level of p-AMPK and a lower level of p-mTOR relative to those in the model group (Figure 3). Significant differences in the protein levels of p-AMPK and p-mTOR were observed between the two groups (p<0.05) (Figure 4).

Expression Level of mRNAs Determined Via qPCR

The expression level of miR-29 was significantly higher in the normal group than that in the model group, and the difference was statistically significant (p<0.05, Figure 5), indicating that miR-29 expression is down-regulated in the retinas of mice with diabetic retinopathy.

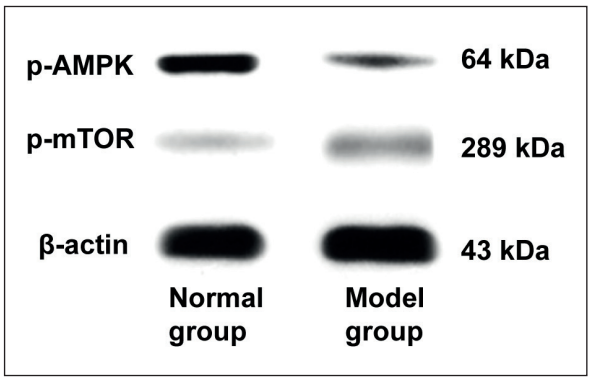

Figure 3. Protein expressions detected via Western blotting.

Electroretinograms

The latent period of b-wave in the normal group was (57.12±8.11) ms and the mean amplitude was (77.78±7.67) μV, while those in the model group were (81.32±6.83) ms and (42.88±6.11) μV, respectively (Figure 6). Compared with those in the normal group, the latent period and amplitude of b-wave in the model group were substantially prolonged and lowered, respectively, displaying statistically significant differences (p<0.05).

Apoptosis Rate Measured Via TUNEL Assay

The normal group exhibited a lower apoptotic rate than that of the model group. Compared with that in the normal group, the apoptotic rate in the

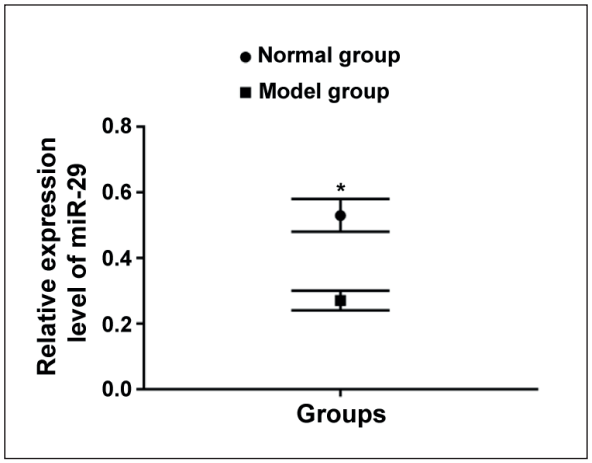

Figure 5. Relative expression level of miR-29. Note: p*<0.05, *vs.* normal group.

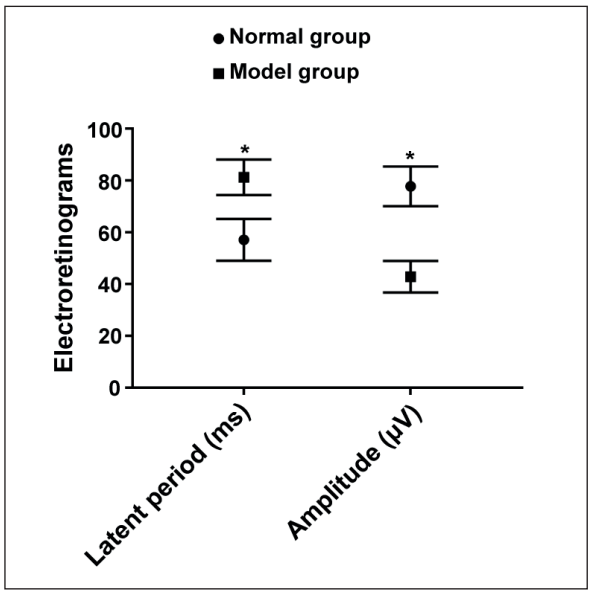

Figure 6. Electroretinograms. Note: p*<0.05, *vs.* normal group.

model group was markedly decreased, and the difference was statistically significant (p<0.05) (Figure 7).

Discussion

Diabetic retinopathy, as one of the important ocular complications of type 2 diabetes, easily leads to blindness and other serious consequences. The 5-year incidence rate of diabetic retinopathy is about 44.4%, and it is predicted that approximately 300 million diabetes patients will experience diabetic retinopathy throughout the world by 2030[6,7]. Recent studies[8,9] have manifested that diabetic retinopathy is the retinal degeneration caused by local retinal microangiopathy invading to the ocular microvessel, which eventually impairs retinal cell function. At the early stage of diabetic retinopathy, functional abnormalities and structural changes are observed in the retinas, which can be effectively diagnosed by electroretinogram. An electroretinogram is a complex wave formed by electrical signals which are generated by the bipolar cells, photoreceptor cells and ganglion cells in the retina under the stimulation by light[10,11]. B-wave, as an important waveform in the electroretinogram, is emitted from bipolar cells and Mueller cells and closely related to the diabetes-induced changes in retinal functions. It can reflect the retinal functions of diabetic patients well[12,13]. This study revealed that the latent period of b-wave in diabetic mice

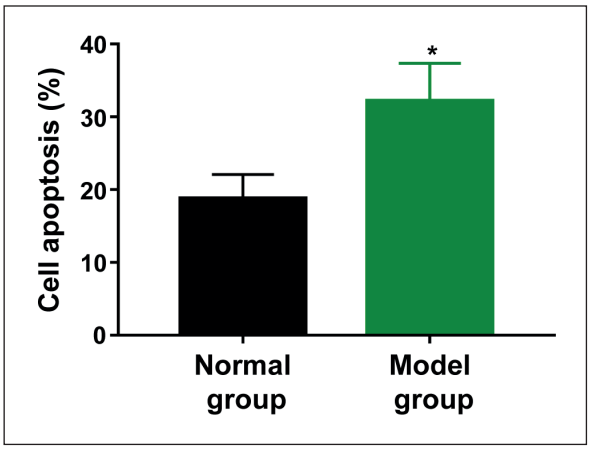

Figure 7. Cell apoptosis detected via TUNEL. Note: p*<0.05, *vs.* normal group.

was significantly prolonged, but the amplitude was remarkably lowered, suggesting that the diabetic mice suffered from retinopathy and retinal function impairment. Cell apoptosis is one of the important pathological responses to diabetic retinopathy, and substantially activated apoptotic factors in the retina with diabetic retinopathy[14]. Bax and Bcl-2, as the critical molecules in the cell apoptosis process, exert key regulatory effects on cell apoptosis. Bcl-2 is an important anti-apoptotic protein. Under physiological state, Bcl-2, as the integrated membrane protein of the organelle, tends to be dislocated once being stimulated by apoptosis signals. It interacts with the anti-apoptotic and pro-apoptotic proteins on cell membranes, thus exerting important two-way effects on apoptosis[15,16]. Besides, Bax, a key member of the Bcl-2 protein family, participates in the apoptosis progression and promotes apoptosis. It coordinates with Bcl-2 to maintain the dynamic balance of the apoptotic process[17,18]. This work manifested that the aberrant expressions of Bax and Bcl-2 were detected in the retinal tissues of diabetic mice, with Bax and Bcl-2 expressions abnormally increased and decreased, respectively. Abnormal apoptosis response in retinal cells of diabetes mice further induced diabetic retinopathy. The AMPK/mTOR signaling pathway, a crucial transduction pathway of cell signals, is involved in various responses, such as cell autophagy and apoptosis. Considered to be an essential ability regulator, this pathway serves as a major treatment target for diabetes[19,20]. Studies have demonstrated that, normally, the p-AMPK can inhibit the phosphorylation of mTOR and regulate the AMPK/mTOR signaling pathway, thereby causing cell autophagy and repressing the pathological reaction of

cell apoptosis. This work revealed that the expression level of p-AMPK in the retinal tissues of diabetic mice notably decreased, but p-mTOR was up-regulated. We believed that in diabetic retinopathy, the inhibited p-AMPK up-regulated phosphorylated level of mTOR to suppress the normal autophagy of dysregulated retinal cells, thus aggravating retinal injuries. Meanwhile, it is considered that miR-29, a kind of non-coding RNA, can regulate the phosphorylation of multiple essential proteins in the cell signal pathways. AMPK, as the target protein of miR-29, can be regulated by miR-29 to modulate several downstream signaling pathways, including the AMPK/mTOR signaling pathway. According to this study, the transcription level of miR-29 in the retinas of diabetic mice was remarkably suppressed. The down-regulation of miR-29 was closely associated with the inhibited AMPK phosphorylation, thereby leading to the change in the downstream AMPK/mTOR signaling pathway and excessive apoptosis in the retinas of mice with diabetic retinopathy.

Conclusions

We observed that the autophagy was attenuated; therefore, miR-29 regulates the AMPK signaling pathway to influence the cell apoptosis and autophagy in diabetic retinopathy.

Conflict of Interests

The authors declared no conflict of interest.

References

1) Cohen SR, Gardner TW. Diabetic retinopathy and diabetic macular edema. Dev Ophthalmol 2016; 55: 137-146.
2) Kumar B, Gupta SK, Saxena R, Srivastava S. Current trends in the pharmacotherapy of diabetic retinopathy. J Postgrad Med 2012; 58: 132-139.
3) Ting DS, Cheung GC, Wong TY. Diabetic retinopathy: global prevalence, major risk factors, screening practices and public health challenges: a review. Clin Exp Ophthalmol 2016; 44: 260-277.
4) Zeng Y, Yi R, Cullen BR. Recognition and cleavage of primary microRNA precursors by the nuclear processing enzyme Drosha. EMBO J 2005; 24: 138-148.
5) Lee Y, Ahn C, Han J, Choi H, Kim J, Yim J, Lee J, Provost P, Radmark O, Kim S, Kim VN. The nuclear RNase III Drosha initiates microRNA processing. Nature 2003; 425: 415-419.
6) Hernandez C, Bogdanov P, Sola-Adell C, Sampedro J, Valeri M, Genis X, Simo-Servat O, Garcia-Ramirez M, Simo R. Topical administration of DPP-IV inhibitors prevents retinal neurodegeneration in experimental diabetes. Diabetologia 2017; 60: 2285-2298.
7) Hernandez C, Garcia-Ramirez M, Corraliza L, Fernandez-Carneado J, Farrera-Sinfreu J, Ponsati B, Gonzalez-Rodriguez A, Valverde AM, Simo R. Topical administration of somatostatin prevents retinal neurodegeneration in experimental diabetes. Diabetes 2013; 62: 2569-2578.
8) Valverde AM, Miranda S, Garcia-Ramirez M, Gonzalez-Rodriguez A, Hernandez C, Simo R. Proapoptotic and survival signaling in the neuroretina at early stages of diabetic retinopathy. Mol Vis 2013; 19: 47-53.
9) Carrasco E, Hernandez C, Miralles A, Huguet P, Farres J, Simo R. Lower somatostatin expression is an early event in diabetic retinopathy and is associated with retinal neurodegeneration. Diabetes Care 2007; 30: 2902-2908.
10) Fan B, Sun YJ, Liu SY, Che L, Li GY. Neuroprotective strategy in retinal degeneration: suppressing ER stress-induced cell death via inhibition of the mTOR signal. Int J Mol Sci 2017; 18: E201.
11) Chinskey ND, Besirli CG, Zacks DN. Retinal cell death and current strategies in retinal neuroprotection. Curr Opin Ophthalmol 2014; 25: 228-233.
12) Hancock HA, Kraft TW. Oscillatory potential analysis and ERGs of normal and diabetic rats. Invest Ophthalmol Vis Sci 2004; 45: 1002-1008.
13) Nebbioso M, Federici M, Rusciano D, Evangelista M, Pescosolido N. Oxidative stress in preretinopathic diabetes subjects and antioxidants. Diabetes Technol Ther 2012; 14: 257-263.
14) Murakami Y, Notomi S, Hisatomi T, Nakazawa T, Ishibashi T, Miller JW, Vavvas DG. Photoreceptor cell death and rescue in retinal detachment and degenerations. Prog Retin Eye Res 2013; 37: 114-140.
15) Yang L, McBurney D, Tang SC, Carlson SG, Horton WE. A novel role for Bcl-2 associated-athanogene-1 (Bag-1) in regulation of the endoplasmic reticulum stress response in mammalian chondrocytes. J Cell Biochem 2007; 102: 786-800.
16) Saintigny Y, Dumay A, Lambert S, Lopez BS. A novel role for the Bcl-2 protein family: specific suppression of the RAD51 recombination pathway. EMBO J 2001; 20: 2596-2607.
17) Salvador-Gallego R, Mund M, Cosentino K, Schneider J, Unsay J, Schraermeyer U, Engelhardt J, Ries J, Garcia-Saez AJ. Bax assembly into rings and arcs in apoptotic mitochondria is linked to membrane pores. EMBO J 2016; 35: 389-401.
18) Song Y, Zhong M, Cai FC. Oxcarbazepine causes neurocyte apoptosis and developing brain damage by triggering Bax/Bcl-2 signaling pathway mediated caspase 3 activation in neonatal rats. Eur Rev Med Pharmacol Sci 2018; 22: 250-261.
19) Kang MR, Park SK, Lee CW, Cho IJ, Jo YN, Yang JW, Kim JA, Yun J, Lee KH, Kwon HJ, Kim BW, Lee K, Kang JS, Kim HM. Widdrol induces apoptosis via activation of AMP-activated protein kinase in colon cancer cells. Oncol Rep 2012; 27: 1407-1412.
20) Kang MR, Park SK, Lee CW, Cho IJ, Jo YN, Yang JW, Kim JA, Yun J, Lee KH, Kwon HJ, Kim BW, Lee K, Kang JS, Kim HM. Widdrol induces apoptosis via activation of AMP-activated protein kinase in colon cancer cells. Oncol Rep 2012; 27: 1407-1412.